

Electrochemical and Neutron Reflectivity Studies of Spontaneously Formed Amphiphilic Surfactant Bilayers at the Gold–Solution Interface

V. Zamlynyy, I. Burgess, G. Szymanski, and J. Lipkowski*

Department of Chemistry and Biochemistry, University of Guelph, Guelph, Ontario N1G 2W1, Canada

J. Majewski, G. Smith, S. Satija, and R. Ivkov

Manual Lujan, Jr. Neutron Scattering Center–12, Los Alamos National Laboratory, Los Alamos, New Mexico 87545, and National Institute of Standards and Technology Center for Neutron Research, National Institute of Standards and Technology, Gaithersburg, Maryland 20899-8562

Received January 10, 2000. In Final Form: June 22, 2000

We have employed electrochemical and neutron reflectivity measurements to study the transfer of 4-pentadecyl-pyridine (C15–4Py), an insoluble amphiphilic surfactant, from the gas–solution (G–S) interface to the metal–solution (M–S) interface of a Au(111) electrode. Neutron reflectivity experiments have demonstrated that C15–4Py forms a bilayer at the Au(111) electrode surface. Electrochemical experiments demonstrated that this bilayer is formed spontaneously when the electrode surface is brought in contact with the film-covered G–S interface. The surfactant molecules can move from the G–S to the M–S interface across the triple-phase boundary formed where the metal, solution, and gas phases are in contact. Time-dependence experiments have shown that the spreading process is irreversible. Having formed a bilayer or monolayer at the M–S interface, the C15–4Py surfactant molecules do not move back to a film-free G–S interface. Three models were used to analyze the kinetics of spreading. Our results are best explained assuming that the spreading is a first-order surface reaction controlled by the activation barrier that the surfactant molecules have to overcome when crossing the triple-phase line.

Introduction

The objective of this work was to investigate the spontaneous transfer of amphiphilic surfactants spread at the gas–solution (G–S) interface to the solid–solution interface of a gold electrode. The solid electrode was brought in contact with the gas–solution interface using the horizontal-touch (Langmuir–Schaefer) technique. In this geometry, the edge of the electrode surface forms a three-phase boundary between solid, liquid, and gaseous phases. Surfactant molecules must cross this triple-phase line if they are to exchange between the G–S and the metal–solution (M–S) interfaces. Previously,^{1–5} we have investigated films of amphiphilic surfactants transferred to the M–S interface using differential-capacity and charge-density measurements. These experiments were completed in a time scale on the order of minutes. Within this short experimental time, we observe no evidence of surfactant molecules crossing the triple-phase line. We have concluded that once it is deposited on the metal electrode surface, the film at the M–S interface is not affected by a change in the physical state of the film spread at the G–S interface.^{2,3}

Steel et al.⁶ recently reported that Langmuir monolayers can flow across the triple-phase line to the M–S interface

of an organothiol-modified gold electrode. Independently, we presented preliminary results⁷ to show that 4-pentadecyl-pyridine (C15–4Py) surfactant can spread from the G–S to the M–S interface of a Au(111) electrode to form a bilayer. In the present work, we will provide a detailed description of the spontaneous transport of C15–4Py molecules across the triple-phase line, using the results of differential-capacity and charge-density measurements. We will also discuss the results of neutron reflectivity experiments used to describe the structure of this film.

We will also show that the slow rate of molecular migration requires over 8 h before the interface becomes saturated with bilayer coverage of surfactant molecules. This slow rate explains why the transfer of insoluble surfactants from the G–S to the M–S interface was not observed in previous, short-duration experiments.^{1–5} We will describe an interesting case of an exchange of mass between multiple two-dimensional phases and provide significant new information about the mechanism by which amphiphilic surfactants spontaneously self-assemble at the solid–solution interface. This knowledge is relevant for tribology and biomimetic research, as well as far the development of sensors and biosensors.

Experimental Section

Reagents, Solutions, and Electrode Materials. A gold single crystal in the shape of a hemisphere, prepared as described in ref 8, was used as a working electrode. The flat base of this

(7) Bizzotto, D.; Zamlynyy, V.; Burgess, I.; Jeffrey, C.A.; Li, H.-Q.; Rubinstein, J.; Galus, Z.; Nelson, A.; Pettinger, B.; Merrill, A.R.; Lipkowski, J. *Amphiphilic and Ionic Surfactants at Electrode Surfaces. In Interfacial Electrochemistry, Theory, Experiment and Applications*; Wieckowski, A., Ed.; Marcel Dekker: New York, 1999.

* To whom correspondence should be addressed.

(1) Bizzotto, D., Noël, J.; Lipkowski, J. *Thin Solid Films* **1993**, *248*, 69.

(2) Bizzotto, D., Noël, J. J.; Lipkowski, J. *J. Electroanal. Chem.* **1994**, *369*, 259.

(3) Bizzotto, D.; Lipkowski, J. *J. Electroanal. Chem.* **1996**, *409*, 33.

(4) Bizzotto, D.; Lipkowski, J. *Progress Surf. Sci.* **1996**, *50*, 237.

(5) Bizzotto, D.; Lipkowski, J. *Prog. Colloid Polym. Sci.* **1997**, *103*, 201.

(6) Steel, A. B.; Cheek, B. J.; Miller, C. J. *Langmuir* **1998**, *14*, 5479.

hemisphere in the shape of a disk (0.35 cm in diameter) constituted the (111) plane of the single crystal. Before each experiment the working electrode was flame-annealed, cooled first in air and then in water, and transferred to the electrochemical cell under protection of a water drop covering its surface. A flame-annealed gold coil was used as a counter electrode. The reference electrode was an external saturated calomel electrode (SCE) connected to the electrochemical cell by means of a salt bridge. All potentials reported in this paper were measured with respect to the SCE.

Milli-Q water of resistivity higher than 18 M Ω was used to wash the cell and to prepare all the aqueous solutions. KClO₄ (ACS-certified AESAR) used to prepare 0.05 M solution of working electrolyte had been calcinated at 300 °C and twice recrystallized before use. Suprapure KHCO₃ (BDH Analar, England) was used without further purification to prepare a 0.4 M aqueous solution. This solution was added with the use of a clean glass pipet (~0.1 mL) to the electrolyte in the cell (~40 mL) to obtain a 0.001 M solution of KHCO₃ and a constant pH ~ 9. Adding KHCO₃ to electrolyte shifted the hydrogen evolution to more negative potentials, allowing complete desorption of the film to take place before the onset of the hydrogen evolution reaction. In addition, adding KHCO₃ suppressed protonation of the pyridine moiety of the surfactant molecule (for pyridine, pK_a = 5.25).

4-Pentadecyl-pyridine (C15-4Py) was synthesized and purified by A. McAlees and R. McCrindle as described in ref 9. C15-4Py (8 mg) was dissolved in 5 mL of chloroform (ACS certified, spectroscopy grade, Fisher) to produce a 5.5 mmol/L stock solution of the surfactant. All the glassware used in the experiment was washed in a 1:3 mixture of nitric and sulfuric acids and rinsed in Milli-Q water.

Electrochemical Measurements and Instrumentation.

After being assembled and filled with electrolyte, the cell was deaerated with argon (BOC gases). The working electrode was introduced under the protection of a water drop and positioned in a hanging meniscus configuration. Initial measurements such as cyclic voltammetry, cyclic ac voltammetry, and chronocoulometry were performed to characterize the bare surface of the electrode and to check the cleanliness of the electrolyte. If the interface was found to be clean, 0.1 mL of the 0.4 M stock KHCO₃ solution was added to the cell, and its contents were purged and mixed with argon by bubbling the gas through the working electrode for 5 min. The cleanliness of the interface was then retested. If the interface remained clean, the working electrode was withdrawn, reannealed, and reintroduced (dry) into the cell to cool in an argon atmosphere. Approximately 8 μ L of the surfactant solution was spread at the surface of the electrolyte, using a 10 μ L syringe (Hamilton). Small droplets of the surfactant solution were delivered onto the electrolyte surface, until the last drop formed a lens that remained stable for at least 1 min. The surfactant film, deposited on the gas-solution interface, maintained a constant equilibrium spreading pressure (ESP) of 33 mNm⁻¹ throughout the whole experiment. The film pressure was determined in a separate experiment using a Wilhelmi plate. To transfer the surfactant spread at the G-S interface to the M-S interface, the dry working electrode was slowly brought to the electrolyte surface and placed in contact with the surfactant film. The surface of the electrode was preadjusted to be parallel to the surface of the electrolyte, and the working electrode potential was preset to 0 V (SCE). After the deposition, the working electrode was elevated (ca. 2 mm) to assume a hanging meniscus configuration, and the electrochemical characterization of the surfactant-covered Au(111) surface was carried out.

A Heka potentiostat and PAR model 129A lock-in amplifier were used to measure and control the electrical variables of the interface. Data were digitized via an RC Electronics acquisition board and processed by a computer. The differential capacity of the interface was measured by superimposing a small ac perturbation of 5 mV rms and 25 Hz on a 5 mV/sec voltage ramp. The in-phase and out-of-phase components of the ac current were then measured using a lock-in amplifier. Differential capacity was calculated assuming a simple series RC equivalent circuit.

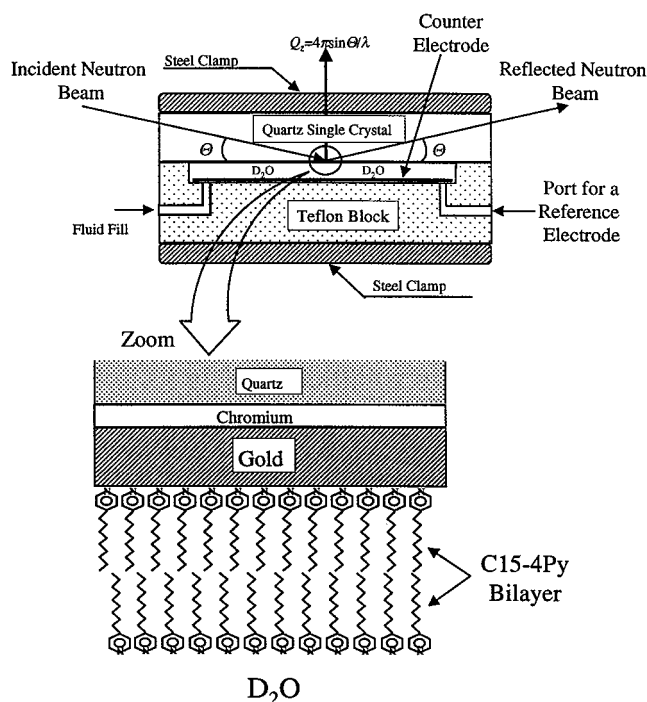


Figure 1. Diagram of the liquid-solution interface cell used for neutron-reflectivity measurements. The neutron beam travels through the quartz substrate and is reflected at the solid-solution interface by the organic layer immersed in D₂O. The zoom shows a schematic representation of the film of surfactant molecules at the solid-solution interface. The first layer of C15-4Py molecules is turned with the pyridine moiety next to the metal, while the pyridine polar heads in the second layer are hydrogen-bonded to the D₂O phase.

Chronocoulometry was used to measure the charge density at the M-S interface. The procedure described in ref 10 was used to measure the charge densities.

Neutron Reflectivity Measurements. Monocrystalline quartz substrates used for reflectometry were purchased from CrysTec GmbH (Berlin, Germany) and were polished to rms roughness of about 5 Å as checked by X-ray reflectivity. A thin layer of about 30 or 60 Å of chromium and a layer of about 74 or 103 Å of gold were sputtered on the monocrystalline quartz substrates in a vacuum. D₂O (99.9%) from Sigma (St. Louis, MO) was used as a solvent in reflectivity studies. The electrode was cleaned in warm concentrated sulfuric acid and rinsed with Milli-Q water. A film of C15-4Py at the ESP was transferred from the air-solution interface to a dry gold-coated surface of the quartz substrates, using the Langmuir-Schaefer technique. The electrode was then mounted on a special cell made of Teflon and schematically shown in Figure 1. The cell had ports for the counter (gold foil) and reference electrodes (Ag/AgCl, E = 45 mV versus SCE). The contact between the gold-coated surface of the quartz substrate (working electrode) and a lead to the potentiostat was achieved using a spring-loaded steel bar. The resistance of the thin film of gold was on the order of a few ohms.

The neutron reflectivity measurements were made on the NG-7 reflectometer at the National Institute of Standards and Technology (NIST) at room temperature (20 ± 2 °C). The neutron reflectivity measures the normalized (by the incident flux) intensity of specularly reflected neutrons *R* as a function of the momentum transfer vector *Q_z* ($Q_z = 4\pi \sin \theta / \lambda$, where θ is the angle of incidence and λ is the wavelength of neutrons). A fixed neutron wavelength of 4.75 Å was used. The measured *Q_z* range from ~0.0 to about 0.14 Å⁻¹ was achieved by varying the angle of incidence. Reflectivities *R* with reasonable statistics were measured down to values $R \sim 10^{-5}$. Typical counting times were 3 h. The reflected neutrons were counted using a ³He detector. The data were reduced (taking into account the neutron beam

(8) Richer, J.; Lipkowski, J. *J. Electrochem. Soc.* **1986**, *133*, 121.

(9) Bizzotto, D.; McAlees, A.; Lipkowski, J.; McCrindle, R. *Langmuir* **1995**, *11*, 3243.

(10) Sagara, T.; Zamlynyy, V.; Bizzotto, D.; McAlees, A.; McCrindle, R.; Lipkowski, J. *Isr. J. Chem.* **1997**, *37*, 197-211.

transmission through the quartz substrate) and corrected for the background. The error points on the data represent the statistical errors in the measurements (standard deviation, σ_R). A constant instrumental resolution of $\Delta Q_z/Q_z = 0.043$ (fwhm) was used throughout the scan. An “inverted” geometry, shown in the zoomed section in Figure 1, in which the gold-coated quartz electrode was above D_2O phase, was used in our experiments. In this case, the lower medium (D_2O) had higher scattering-length density than the upper one. Under these conditions, the reflectivity R is approximately 1 for Q_z below a critical value $Q_c = 4(\pi\Delta\beta)^{1/2}$, where $\Delta\beta$ is the scattering-length density difference between the lower and the upper media. Above Q_c , R decays as a function of Q_z , and the character of this decay depends on the area-averaged scattering-length density profile normal to the interface.

Results and Discussion

Spreading of C15–4Py to a Monolayer-Coated Electrode Surface. The metal–electrolyte interface has the properties of a capacitor. It is well-known that the capacitance of the interface decreases when organic molecules are adsorbed at the metal surface.¹¹ Therefore, measurement of the differential capacity provides a convenient means to study the transfer of amphiphilic surfactants to the surface of a metal electrode.^{1–7} Initially, we investigated the transfer of C15–4Py from the gas–solution interface, across the triple-phase line, to the metal surface that was coated with a monolayer of the pyridine surfactant. Effectively, we have studied a spontaneous transformation of a monolayer into a bilayer, because of the transfer of C15–4Py molecules from the G–S to the M–S interface covered with a film of C15–4Py that was predeposited using the single-horizontal-touch method. This case resembled the flow of Langmuir monolayers to the organothiol-modified gold surface described by Steel et al.⁶

A monolayer film of C15–4Py was spread at the gas–solution interface of an electrochemical cell at the equilibrium spreading pressure (33 mN m^{-1}). The film at the electrolyte surface was then brought in contact with the (111) surface of a gold electrode at a controlled potential $E = 0 \text{ V}$ (SCE), using the horizontal-touch method. The differential capacity of the interface was measured immediately after the contact had been established. At a potential of 0 V (SCE), the capacity of the interface assumed a value between 8 and $5 \mu\text{F/cm}^2$, significantly lower than the capacity of the film free gold–solution interface (ca. $34 \mu\text{F/cm}^2$ at 0 V and $\text{pH} \sim 9$). This feature indicates that the film of C15–4Py was transferred to the electrode surface during the horizontal-touching procedure.

A slow voltage ramp was then applied to the electrode surface, and the capacity curve, shown as a solid line in Figure 2, was recorded. The shape of this curve is consistent with the results described earlier.¹⁰ When the potential moves in a negative direction a maximum at $E \sim -0.2 \text{ V}$ (SCE) can be seen. This maximum indicates a phase transition in the organic film. When the potential is moved further in the negative direction, the capacity increases until, at $E \leq -0.8 \text{ V}$ (SCE), it becomes equal to the capacity of the film-free electrode. This behavior indicates that the film is desorbed from the electrode surface at negative potentials. When the direction of the voltage sweep is reversed, the capacity decreases, and at $E \sim 0 \text{ V}$ it attains the initial value of about $8 \mu\text{F/cm}^2$. Apparently, the film reforms on the gold surface. At potentials higher than 0.3 V (SCE), the capacity rises again. This increase indicates the onset of film desorption,

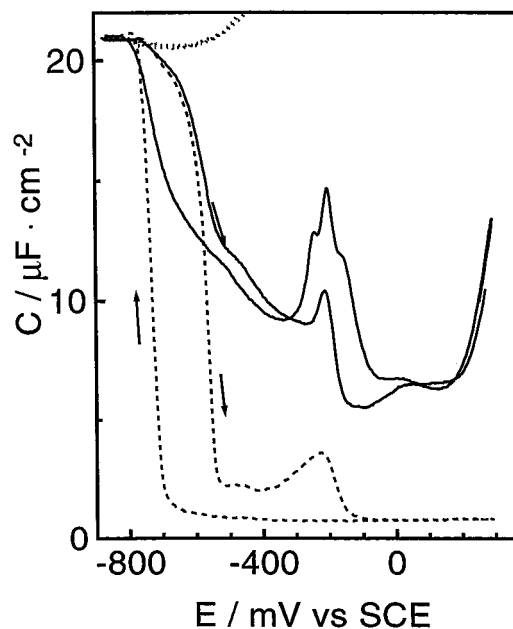


Figure 2. Differential capacity of the Au(111) electrode dotted line; film-free interface; solid line, interface covered with a film of C15–4Py molecules deposited at $E = 0 \text{ V}$ using the single-horizontal-touch procedure. The curve was recorded immediately after contact was made between the electrode and the film-covered gas–solution interface. Dashed line, interface covered by a film produced by spontaneous transfer of C15–4Py molecules from the gas–solution to the metal–solution interface after 18 h of equilibration time. The electrolyte solution was $50 \text{ mM KClO}_4 + 1 \text{ mM KHCO}_3$.

most likely promoted by a competitive adsorption of hydroxide and/or bicarbonate ions. Gold oxide formation prevents further extension of electrode potentials in the positive direction.

Light-scattering and fluorescence quenching experiments described in refs 9 and 10 demonstrated that C15–4Py desorbed from the electrode surface at $E \leq -0.8 \text{ V}$ is trapped in the vicinity of the electrode surface in the form of micellar aggregates which fuse back onto the metal surface when the electrode potential is made less negative. The hysteresis on the differential capacity curve indicates that desorption and film-reformation processes are slow on the time scale of the voltage ramp (5 mV/s). It may also indicate that desorption of the film from the electrode surface and fusion of aggregates onto the surface may involve different mechanisms. However, independent potential step experiments indicate that the film can be reformed completely within a time window of 90 s .¹⁰ For the purpose of the subsequent experiment, it is important to stress that the film, initially deposited at the gold electrode surface at $E = 0 \text{ V}$, may be desorbed at negative potentials and then completely recovered by changing the potential back to 0 V . The film-desorption and recovery processes require time on the order of minutes. The properties of the film are not changed by the desorption and reformation cycle.

When the film-covered electrode was allowed to equilibrate with the monolayer of C15–4Py spread at the electrolyte surface, at a constant potential of 0 V , for 18 h , the differential capacity of the electrode was measured in intervals. Figure 3 shows the differential-capacity curves determined for different equilibration times. For the sake of clarity, only sections recorded during the positive voltage sweep are presented in this figure. Apparently, the capacity decreases with the equilibration time until it approaches a steady-state value after 8 h .

(11) Damaskin, B.B.; Petrii, O.A.; Batrakov, V.V. *Adsorption of Organic Compounds on Electrodes*; Plenum Press: New York, 1971.

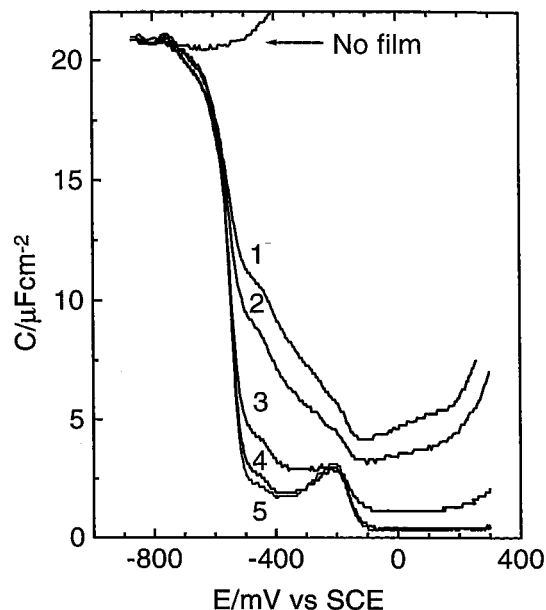


Figure 3. Evolution of the differential capacity of the Au(111) electrode with equilibration time between the film of C15-4Py molecules at the gold-solution interface and the gas-solution interface of the electrochemical cell. The number associated with each curve corresponds to the following equilibration times: 1, 0 h, curve recorded just after the contact was made between the electrode surface and the film-covered gas-solution interface; 2, 1 h; 3, 4 h; 4, 6 h; 5, 8 h. For clarity, only the portions of the differential-capacity curves recorded during the positive voltage sweep are shown. The supporting electrolyte solution was 50 mM KClO_4 + 1 mM KHCO_3 .

The full differential-capacity curve recorded after 18 h of the experiment is plotted as a dashed curve in Figure 2. The differential-capacity curves determined after 8 and 18 h of equilibration are very close. The progressive decrease of the differential capacity with the equilibration time indicates that the amount of C15-4Py molecules at the metal-solution interface increases with time. This behavior strongly suggests that C15-4Py molecules are transported across the triple-phase line from the gas-solution interface to the gold-solution interface.

In fact, the differential-capacity curves recorded after 8 or 18 h of equilibration resemble the curve recorded for the electrode covered by a film produced by the double horizontal touch method.^{9,10} In the double-horizontal-touch experiment, the electrode, covered by a film of surfactant, is removed from the solution surface and horizontally touched for a second time to the surfactant-covered gas-solution interface. Neutron reflectivity experiments, described below, demonstrated that the monolayer of C15-4Py remains on the electrode surface when the initially covered electrode is removed from the solution, and that a bilayer film is formed by the double-touch procedure. Hence the bilayer of C15-4Py is formed after a sufficiently long equilibration time. Indeed, for potentials higher than -0.1 V, the capacity of the interface recorded after 18 h of equilibration or after the double-horizontal-touch procedure has a very small value of about $0.8 \mu\text{F}/\text{cm}^2$, which is characteristic of a bilayer. The pyridine moiety of the surfactant molecule can interact relatively strongly with the gold surface.^{12,13} Consequently, in the first

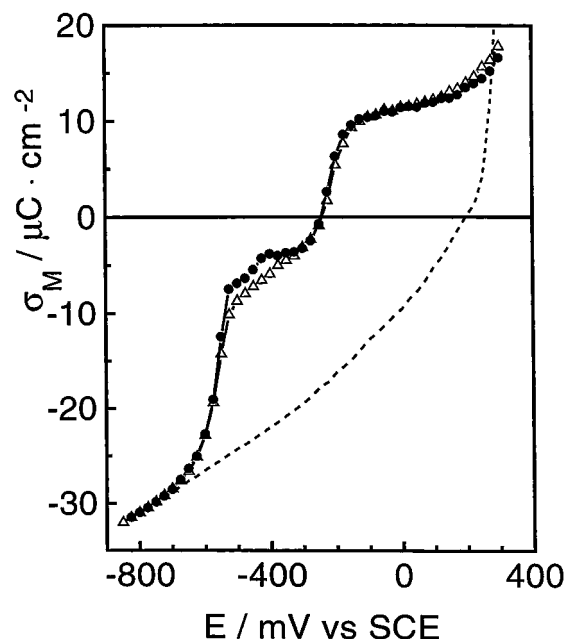


Figure 4. Charge density of the Au(111) electrode: dashed line, film-free interface; open triangles, in the presence of a film obtained using the single-horizontal-touch at $E = 0$ V followed by 18 h of equilibration with the film at the gas-solution interface; solid circles, in the presence of a film obtained at $E = 0$ V using the double-horizontal-touch procedure. The supporting electrolyte solution was 50 mM KClO_4 + 1 mM KHCO_3 .

monolayer, C15-4Py molecules are oriented with the nitrogen heteroatom of the pyridine ring toward the surface and the hydrocarbon tail toward the solution,¹⁰ and hence the metal-solution interface becomes hydrophobic. The second layer of molecules diffuses or flows onto this hydrophobic substrate.

For a quantitative comparison between the film produced by the prolonged equilibration of the electrode with the surfactant spread at the gas-solution interface and the film obtained by the double-horizontal-touch method, it is convenient to analyze the charge-density data. The charge-density plots determined for the Au(111) electrode covered by the two films are compared in Figure 4. These curves were acquired by stepping the potential from a more positive E , where the surfactant molecules are spread at the electrode surface, to a base value of -0.825 V, where the desorbed surfactant molecules form micelle-like aggregates in the vicinity of the electrode surface. In the presence of the surfactant, the charge-density plots display two steps. The nature of these steps has been discussed previously.¹⁰ The first step, at $E = -0.6$ V, corresponds to the adsorption of micellar aggregates onto the electrode surface. The second, at -0.2 V, corresponds to a phase transition in the film that most likely involves spreading of surface hemimicellar aggregates into a condensed film. For the purpose of the present discussion, it is important to note the remarkable similarity of the charge-density curves determined for films that were produced by the double-horizontal-touch and the prolonged equilibration procedures. Compared to the film formed by prolonged equilibration, the charge-density data for the film produced by the double-touch method are slightly higher at potentials around -0.4 V and somewhat lower at $E > 0$ V. These small differences may suggest that the film formed by the spontaneous transfer of C15-4Py molecules is slightly less compact than the film produced by the double-touch method. Apart from these minor differences, the similarity of the two

(12) Stolberg, L.; Morin, S.; Lipkowski, J.; Irish, D.E. *J. Electroanal. Chem.* **1991**, *307*, 241-262.

(13) Lipkowski, J.; Stolberg, L. Molecular Adsorption at Gold and Silver Electrodes. In *Adsorption of Molecules at Metal Electrodes*; Lipkowski, J., Ross, P. N., Eds.; VCH Publishers: New York, 1992; pp 171-238.

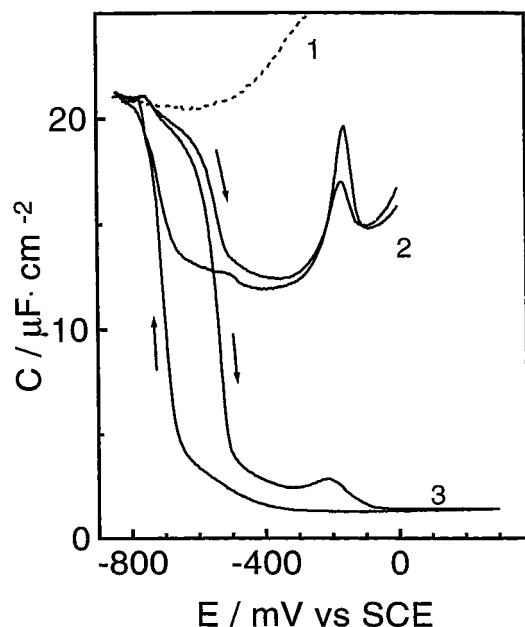


Figure 5. Differential capacity of the Au(111) electrode in contact with surface of electrolyte covered with a C15–4Py film at the equilibrium spreading pressure: 1, curve recorded after contact was made between the electrode and the gas–solution interface; 2, curve recorded after 3.5 h; 3, curve recorded after 18 h. The supporting electrolyte solution was 50 mM KClO₄ + 1 mM KHCO₃.

charge-density curves corresponding to the two films strongly suggests that the C15–4Py molecules cross the triple-phase line to form a bilayer at the gold–solution interface.

Spreading of C15–4Py onto the Film-Free Electrode Surface. In the preceding section, we described the transformation of a monolayer of chemisorbed surfactant to a bilayer. This transformation resulted from the spontaneous transfer of the surfactant molecules from the gas–solution interface to the monolayer-covered metal–solution interface. The following experiment was performed to test whether C15–4Py molecules will also move from the G–S interface to an initially surfactant-free M–S interface. The Au(111) electrode was flame-annealed and then quenched with water. The drop of water adhered to the clean electrode surface. This electrode was brought in contact with the film of surfactant molecules spread on the electrolyte surface. The initial presence of the water droplet prevented transfer of the surfactant film to the electrode surface. However, as soon as contact between the M–S and G–S interfaces was achieved, the differential capacity revealed the onset of surfactant spreading on the metal surface. The electrode was then allowed to equilibrate with the film at the G–S interface for a period of 18 h. The differential capacity of the gold–solution interface was recorded every few hours to monitor the transfer of C15–Py molecules from the G–S to the M–S interface.

The results of these measurements are shown in Figure 5. The differential capacity of the interface, recorded immediately after the electrolyte surface was touched, was characteristic of a film-free Au(111) surface. However, the differential-capacity curve recorded after 3.5 h of equilibration time was already reminiscent of the curve recorded for the monolayer-covered surface, indicating that surfactant molecules move from the G–S to the M–S interface through the triple-phase line. After a prolonged waiting time of 18 h, the differential capacity of the M–S interface decreased further, and the differential-capacity

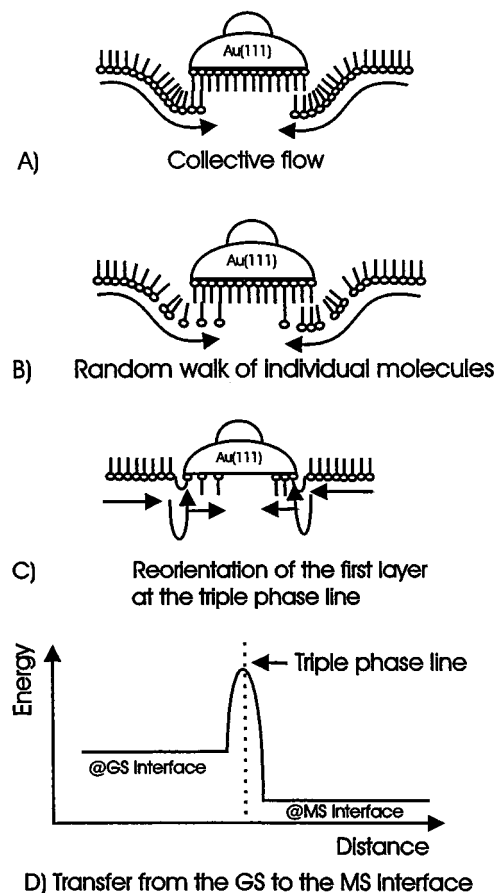


Figure 6. Schematic models of different mechanisms describing mass transfer from the G–S to the M–S interface. (a) Film-pressure-driven viscous flow of a Langmuir monolayer (“collective flow”) to a hydrophobic surface; (b) free-volume model of lateral diffusion (“random walk”) to a hydrophobic surface; (c) generalized model for mass transport to a film-free surface involving reorientation of the surfactant headgroup; (d) schematic description of the free energy profile of a transfer of an insoluble surfactant molecule from the G–S to the M–S interface.

curve became quite similar to that recorded for the Au(111) surface covered with the film obtained by the double-touch procedure. This experiment indicates that C15–4Py molecules can spread from the G–S interface not only to the hydrophobic M–S, but also to the film-free gold–solution interface to assemble spontaneously into a bilayer.

Mechanisms. Three mechanisms can be employed to describe the spontaneous spreading of C15–4Py molecules from the G–S to the M–S interface. The first, proposed recently by Steel et al.,⁶ assumes that spreading is caused by a film-pressure-driven viscous flow of the Langmuir monolayer across the triple-phase boundary. The second is the Cohen and Turnbull^{14,15} free-volume model of diffusion in fluids. It describes diffusion in lipid bilayers^{16,17} and was recently applied by Majda and co-workers^{18,19} to study lateral diffusion at the air–water interface. The two models are depicted schematically in Figure 6. We

(14) Cohen, M. H.; Turnbull, D. *J. Chem. Phys.* **1959**, *31*, 1164.

(15) Turnbull, D.; Cohen, M. H. *J. Chem. Phys.* **1970**, *52*, 3038.

(16) Galla, H.-J.; Hartmann, W.; Theilen, U.; Sackmann, E. *J. Membr. Biol.* **1979**, *48*, 215.

(17) Vaz, W. L. C.; Clegg, R. M.; Hallmann, D. *Biochemistry* **1985**, *24*, 781.

(18) Charych, D. H.; Landau, E. M.; Majda, M. *J. Am. Chem. Soc.* **1991**, *113*, 3340.

(19) Lee, W.-Y.; Majda, M.; Brezesinski, G.; Moebius, D. *J. Phys. Chem. B* **1999**, *103*, 6950.

have loosely applied the phrases “collective flow” and “random walk” to differentiate between the viscous-flow and diffusion models. To test these models quantitatively, one must analyze the dependence of the differential capacity on the equilibration time. The differential-capacity curves in Figure 3 display a quite flat minimum at $E = 0$ V (SCE). At this potential, we define the fraction Θ of the metal–solution interface covered by the bilayer in terms of

$$\Theta = \frac{C_0 - C_t}{C_0 - C_\infty} \approx \frac{\Gamma}{\Gamma_\infty} \quad (1)$$

where C_0 , C_t , and C_∞ are the differential capacities at zero equilibration time; at equilibration time, t ; and at infinitely long (18 h) equilibration time, respectively. In the case of spreading on a monolayer-covered metal surface, Θ measures the extent of transformation of the monolayer to the bilayer; in the case of spreading to a bare electrode surface, Θ measures the extent of film formation. In the viscous-flow model, the parameter Θ is related to time by the equation 6

$$\Theta = \sqrt{2k\pi t} \quad (2)$$

where k is a proportionality constant and π is the surface pressure of the film at the G–S interface.

The parameter Θ may also be used as a measure of the fraction of molecules transported to the M–S interface across the triple-phase line (Γ/Γ_∞) by diffusion, where Γ is the surface concentration of molecules transferred to M–S at a given equilibration time t and Γ_∞ is the surface concentration after infinitely long equilibration time.¹¹ The M–S interface is disk-shaped and characterized by radius r_0 . Initially, the surface concentration of C15–4Py, either in the second layer or at the bare M–S interface, is equal to zero $\Gamma(t = 0) = 0$. The diffusion from the G–S to the M–S interface is driven by the gradient of the chemical potential. The film pressure at the G–S interface is equal to the equilibrium spreading pressure during the whole duration of the experiment. Consequently, the surface concentration of C15–4Py outside the disk is uniform and equal to the surface concentration at the triple-phase line $\Gamma(r = r_0)$. The formation of the bilayer is complete when the surface concentration in the second layer of the M–S interface becomes equal to the surface concentration at the G–S interface $\Gamma_\infty = \Gamma(r = r_0)$. The number of molecules crossing a unit length of the triple-phase line during time t is given by²⁰

$$n = \int_0^t D \left(\frac{\partial \Gamma(r)}{\partial r} \right)_{r=r_0} dt \quad (3)$$

To calculate the surface concentration of molecules diffusing to the electrode, one must multiply n by the length of the disk perimeter (length of the triple-phase line), $2\pi r_0$ and to divide the product by the electrode area, πr_0^2 . The result is

$$\Gamma = \frac{2}{r_0} \int_0^t D \left(\frac{\partial \Gamma(r)}{\partial r} \right)_{r=r_0} dt \quad (4)$$

It is difficult to find an analytical solution of this equation. For lateral diffusion of a surfactant molecule, the diffusion

(20) Buess-Herman, Cl. Dynamics of Adsorption and Two-Dimensional Phase Transitions at Electrode Surfaces. In *Adsorption of Molecules at Metal Electrodes*; Lipkowsky, J., Ross, P. N., Eds.; VCH Publishers, New York, 1992; p 79.

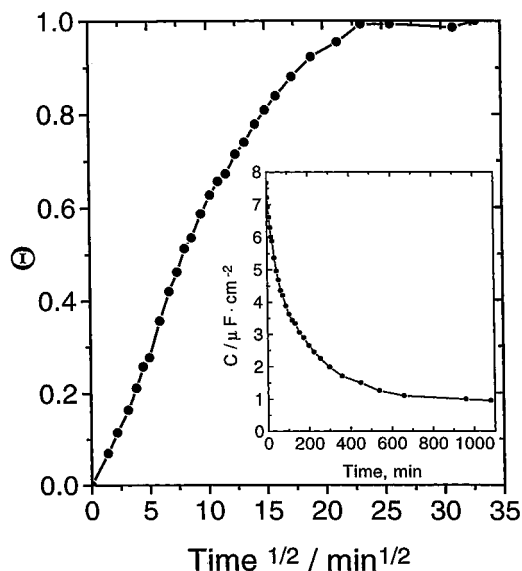


Figure 7. Extent of transformation of the monolayer into a bilayer, plotted against the square root of equilibration time between the films spread at the metal–solution and the gas–solution interfaces. Inset: dependence of the differential capacity on the equilibration time. The supporting electrolyte solution was 50 mM KClO_4 + 1 mM KHCO_3 .

coefficient depends on the surface concentration Γ . That dependence was described by Majda and co-workers.¹⁸ In addition, the diffusion to the disk surface is a diffusion into a limited-space, and solutions for diffusion under limited-space conditions are complex.²¹ However, we can provide an estimate of the initial diffusion rate. At the initial stage of diffusion, one can treat the disk as a semi-infinite space. In addition, at the initial stage we will consider the diffusion coefficient to be coverage-independent.²² The flux of molecules across the disk perimeter may then be described by the Cottrell equation:

$$D \left(\frac{\partial \Gamma(r)}{\partial r} \right)_{r=r_0} = D \frac{\Gamma_{r=r_0}}{\sqrt{\pi D t}} \quad (5)$$

and the initial change of the fraction Θ with time may be described by

$$\Theta = \frac{\Gamma}{\Gamma_{r=r_0}} = \frac{4}{r_0} \sqrt{\frac{D t}{\pi}} \quad (6)$$

We note that both the viscous-flow model and the lateral-diffusion model predict that initially the fraction Θ should vary linearly with the square root of time. We will now use the expressions for viscous flow and lateral diffusion to analyze the variation of Θ with time for the spreading of C15–4Py on both the monolayer-coated and the bare (film-free) electrode surfaces.

For spreading of C15–4Py molecules on the monolayer-covered M–S interface at $E = 0$ V (SCE), the fraction Θ is plotted versus the square root of the equilibration time in the main section of Figure 7. The initial portion ($\Theta < 0.4$) of this plot is linear. At higher fractions of Θ , a

(21) Galus, Z. *Fundamentals of Electrochemical Analysis*, 2nd ed.; Ellis Harwood Ltd.: Chichester, U.K., 1994; p 211.

(22) According to the free-volume model of diffusion,^{15,18} the diffusion coefficient is proportional to the free volume if it is much larger than the minimum void volume necessary for diffusion. In our experiments, the free volume is proportional to $(1 - \Theta)$. Therefore, eq 6 may be used to calculate the diffusion coefficient from the initial slope of the Θ versus \sqrt{t} plot, only when $\Theta \rightarrow 0$.

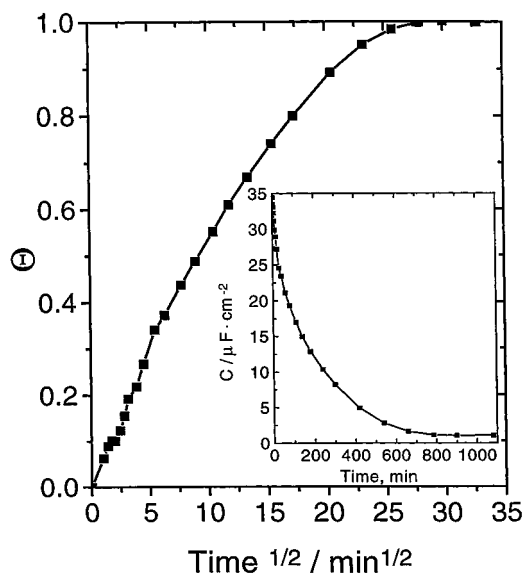


Figure 8. Extent of the bilayer formation on the initially film-free Au(111) electrode surface, plotted against the square root of equilibration time between the films spread at the metal–solution and the gas–solution interfaces. Inset: dependence of the differential capacity on the equilibration time. The supporting electrolyte solution was 50 mM KClO_4 + 1 mM KHCO_3 .

deviation from linearity is observed. The inset in Figure 7 shows how the capacity of the M–S interface at $E = 0$ V changes with the equilibration time. The capacity decreases with time from a value of $\sim 8 \mu\text{F}/\text{cm}^2$ (characteristic of a monolayer-coated gold surface) to a value of $0.08 \mu\text{F}/\text{cm}^2$, representative of a bilayer-covered metal surface. We would like to emphasize that in this experiment C15–4Py molecules of the monolayer that was precoated on the gold surface were oriented with the pyridine moiety toward the metal and the hydrocarbon tail toward the solution. Therefore, the transfer of pyridine molecules from the G–S to the M–S interface could be seen as a sliding of a slab (second monolayer) of C15–4Py molecules from the G–S onto a slab of C15–4Py (first monolayer) attached to the gold surface. The sliding of the two slabs is opposed by frictional tail-to-tail interactions between the surfactant molecules in the two layers.

The kinetics of the spontaneous formation of the bilayer at the bare gold surface is described in Figure 8. Equation 1 was used again to calculate the fraction of the bilayer formation from the capacity data. This time, C_0 represents the capacity of the film-free M–S interface. The fraction Θ is plotted versus the square root of equilibration time in the main section of Figure 8. The inset of the figure shows how the electrode capacity changes as a function of time. In a period of 18 h, the capacity drops from a value of about $34 \mu\text{F}/\text{cm}^2$, characteristic of a film-free interface, to a value of $0.08 \mu\text{F}/\text{cm}^2$, characteristic of a bilayer. In contrast to the previous case, it is difficult to envisage that the transfer of C15–4Py onto the bare electrode surface involves sliding of a monolayer thick slab of the surfactant from the G–S to the M–S interface. The C15–4Py molecules are oriented with the pyridine moiety toward solution at the G–S interface, whereas in the first layer of the bilayer, the pyridine moiety is turned toward the gold surface. When the first layer is formed at the M–S interface, the surfactant molecules must invert upon crossing the triple-phase line, as schematically depicted in Figure 6c.

Therefore, it is quite surprising to observe that the rates of a spontaneous formation of a bilayer on the film-free electrode surface and the flow of C15–4Py onto the

monolayer-precoated electrode are nearly identical. In the viscous-flow model, the kinetics of film transfer is described in terms of the flow parameter FP ,⁶ which in the present case is given by the expression,

$$FP = \left(\frac{d\Theta}{dt^{1/2}} \right) r_0 \quad (7)$$

The flow parameter may be used to calculate the rate of flow, v , in cm/s with the help of the formula⁶

$$v = (FP)^2 / r_0 \quad (8)$$

The initial slopes of Θ versus $t^{1/2}$ plots in Figures 7 and 8 are identical within experimental error. They give the flow parameter $FP = 1.3 \times 10^{-3} \text{ cm s}^{-1/2}$ and the rate of flow $v = 1.0 \times 10^{-5} \text{ cm s}^{-1}$. These numbers are lower by a factor of 2 than the values of FP and v reported for the flow of oleic acid on a gold surface coated by a monolayer of *n*-alkanethiols.⁶

Alternatively, when the transfer of C15–4Py molecules from the G–S to the M–S interface is interpreted in terms of lateral diffusion, eq 6 may be used to calculate the diffusion coefficient from the initial slope of the Θ versus $t^{1/2}$ plot. The diffusion coefficient, calculated from the data presented in Figures 7 and 8, is equal to $3.4 \times 10^{-7} \text{ cm}^2 \text{ s}^{-1}$. This is a quite reasonable value. It represents the diffusion of C15–4Py molecules in a slab of water next to the electrode surface. It is somewhat lower than the diffusion coefficient of a pyridine molecule in the bulk of an aqueous solution ($5 \times 10^{-6} \text{ cm}^2 \text{ s}^{-1}$), and it is comparable to some of the diffusion coefficients observed for surfactants in lipid bilayers¹⁶ and for the octadecylferrocene amphiphile in Langmuir monolayers.¹⁸ Apparently, the analysis of our data gives reasonable results for both the viscous-flow and the lateral-diffusion models.

The viscous-flow and the surface-diffusion models implicitly assume that the activation energy of crossing the triple-phase line is negligibly small. Alternatively, one may envisage that the spreading of C15–4Py molecules is controlled by the energy barrier at the triple-phase line, as shown schematically in Figure 6d, and is essentially a first-order surface reaction. To derive the kinetic expression for this case, it is useful to determine whether the reaction is reversible or irreversible. To test the reversibility of spreading the surfactant molecules, the electrode, covered by the bilayer, was transferred to a separate cell with a surfactant-free G–S interface. The film-free G–S and the bilayer-covered M–S interfaces were then allowed to equilibrate for about 18 h. We expected that C15–4Py molecules would move back to the film-free G–S interface, driven by the gradient of the chemical potential and/or the gradient of the film pressure. The electrode capacity was measured periodically during this extended equilibration time. Curve 1 in Figure 9 shows the observed changes of the electrode capacity. The changes are negligible. During the period of 18 h, the electrode capacity increased only slightly. Apparently, the surfactant molecules did not move back from the M–S to the G–S interface. This behavior is in contrast to the fast transfer of C15–4Py molecules from the G–S to the M–S interface shown by curve 2 in Figure 9. We have performed a similar experiment with the monolayer-covered electrode surface. Curve 3 in Figure 9 shows the change in electrode capacity when the monolayer-covered M–S interface is allowed to equilibrate with the film-free G–S interface. In contrast to our initial expectations, the capacity did not increase with time. Apparently, C15–4Py molecules do not move back to the film-free G–S interface. (The

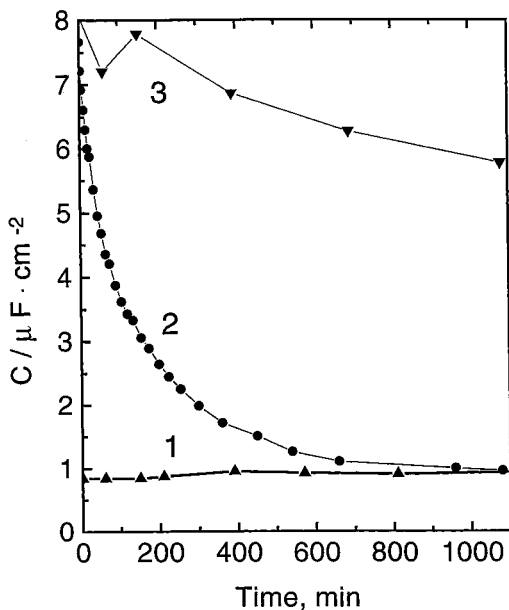


Figure 9. Dependence of the differential capacity of the electrode surface on the equilibration time. Curve 1, M–S interface covered with a bilayer of C15–4Py molecules in equilibrium with the film-free G–S interface. Curve 2, M–S interface covered with a monolayer of C15–4Py molecules in equilibrium with the G–S interface, also covered with a monolayer of C15–4Py molecules at the equilibrium spreading pressure (33 mN m^{-1}). Curve 3, M–S interface covered with a monolayer of C15–4Py molecules in equilibrium with the film-free G–S interface. The supporting electrolyte solution was $50 \text{ mM KClO}_4 + 1 \text{ mM KHCO}_3$.

small decrease of the capacity with time observed in curve 3 probably is due to the migration of C15–4Py molecules from the gas–metal interface to the metal–solution interface.) The above experiments indicate that thermodynamically, both the monolayer and the bilayer of C15–4Py molecules are more favored than the monolayer spread at the G–S interface. At $E = 0 \text{ V}$ (SCE), the formation of the monolayer and the bilayer at the Au(111) surface is irreversible.

If the transfer of surfactant from the G–S to the M–S interface is controlled by the free-energy barrier at the triple-phase line, the change of the coverage with time for this first-order and irreversible surface reaction should be given by

$$\frac{d\Theta}{dt} = k(1 - \Theta) \quad (9)$$

where k is the rate constant, the magnitude of which depends on the activation-energy barrier. Integration of this equation gives a linear relationship between the logarithm of the free area $(1 - \Theta)$ and time:

$$\ln(1 - \Theta) = -kt \quad (10)$$

The experimental data corresponding to the transfer of C15–4Py molecules to the surfactant-free and the monolayer-precoated M–S interface are plotted as $\ln(1 - \Theta)$ versus t in Figure 10. The relationships are nearly linear in a broad range of coverages, from $\Theta = 0.3$ to $\Theta = 0.9$. This behavior indicates that the third mechanism for spreading of the surfactant molecules is also plausible, although it does not describe the experimental results in the whole range of coverages. The rate constants calculated from the slope of the plots in Figure 10 are $6.1 \times 10^{-3} \text{ s}^{-1}$ for the transfer of C15–4Py on a precoated electrode and

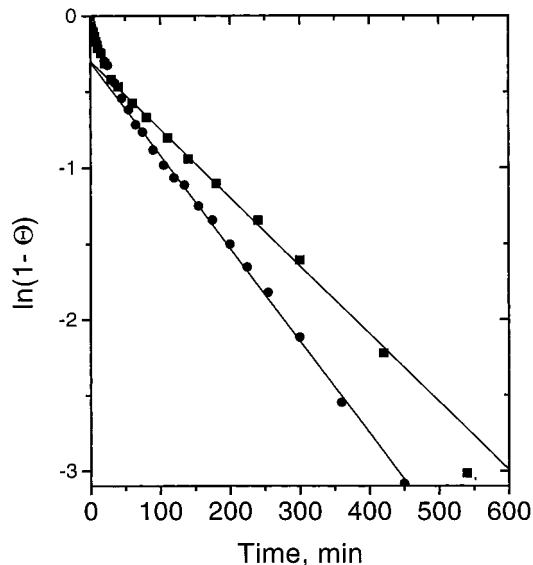


Figure 10. Dependence of the fraction of the film-free electrode area on experiment time. Squares, transfer to the surfactant-free electrode; circles transfer on an electrode precoated with a monolayer of surfactant.

$4.5 \times 10^{-3} \text{ s}^{-1}$ on the surfactant-free electrode. In conclusion, the three mechanisms invoked to discuss the spreading of C15–4Py molecules from the G–S to the M–S interface give a reasonable description of the experimental results. However, similar spreading rates of C15–4Py molecules on the bare and the monolayer-precoated surface are perhaps easier to explain assuming that the rate-determining step consists of overcoming an activation barrier at the triple-phase line.

Neutron-Reflectivity Measurements. Neutron reflectivity measurements were performed to characterize the structure of the monolayer and bilayer of C15–4Py formed at the gold electrode surface. Neutron-reflectivity data allow one to determine the scattering-length density profile perpendicular to the interface. The surface coverage and thickness, as well as the relative position and roughness of individual layers of the film can then be calculated from the scattering-length density profile. Because of the small length scale and the ubiquitous nature of hydrogen in organic assemblies, neutrons are particularly suitable for elucidating structural information regarding these systems. In the case of organic layers at the gold–solution interface, only neutrons can penetrate through the thick (80 nm in our case) substrate and probe the buried structure.

It is difficult to perform neutron-reflectivity measurements on a film of surfactant that was assembled at the gold electrode surface by a spontaneous transfer from the G–S to the M–S interface. Therefore, the neutron-reflectivity experiments were carried out on the monolayer and the bilayer of C15–4Py formed at the gold electrode surface by the single- and the double-touch procedures, respectively. The film was deposited at the open circuit potential (ocp), which was approximately equal to 0 volts versus SCE. Figure 11 shows the neutron-reflectivity curve for the gold electrode covered by a bilayer of C15–4Py. For technical reasons, the reflectivity studies of the monolayer and the bilayer films were performed during different neutron-measurement sessions, using electrodes of different thickness of gold and hence the reflectivity curves for the monolayer and the bilayer films cannot be directly compared. Consequently, only one reflectivity curve is shown in Figure 11. To extract structural information from these data, we analyzed the reflectivities

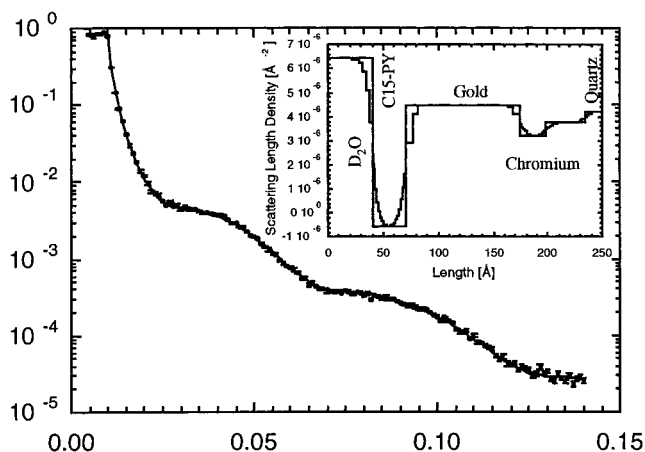


Figure 11. Neutron reflectivity data for the Au electrode covered with C15–4Py film obtained using the double-horizontal-touch technique. The scattering-length density profiles (smeared and unsmeared) are presented in the inset. The numerical values of the fitting parameters are given in Table 1.

using the iterative, dynamic method. The scattering-length densities of chromium, gold, and the organic layers were modeled as boxes of a specified thickness, and one overall root-mean-square roughness factor, σ , was used to smear out all the interfaces. On the basis of facts known about the system (i.e., thickness of the gold and chromium layers and possible structure of the organic layer at the interface), we generated a model reflectivity profile and compared it to the measured reflectivity profile. We then minimized the model using the Marquardt–Levenburg nonlinear least-squares fitting routine, to obtain the best least-squares fit to the data and the most physically reasonable parameters.

Our philosophy was to use the simplest yet most physically reasonable model to fit the experimental data. We began with simple one- or two-box models to account for the Cr and Au layers. If the simple model gave a large χ^2 value, we began to increase its complexity by adding boxes to account for various layers of the interfacial film. The results presented are the best fits to the data that could be obtained using simple, insightful models. Large variations in the parameter space were allowed, but we restricted our models to those that generated reasonable results on the basis of the known lengths and the scattering-length densities of the constituent molecules. This approach enabled us to fit the data with a high level of self-consistency. The parameters of this fit are summarized in Table 1.

To obtain a good fit at the higher-momentum transfer values, we had to divide the scattering-length density box of chromium into two parts. The scattering-length densities of the chromium layers used in the fit ($3.2 \times 10^{-6} \text{ \AA}^{-2}$ and $3.7 \times 10^{-6} \text{ \AA}^{-2}$) are larger than the theoretical value ($3.02 \times 10^{-6} \text{ \AA}^{-2}$). This difference can be the result of a slight mixing of the gold with chromium during the gold-presputtering process. The gold layer is well-described by a single box. The best-fit model of the scattering-length density versus the distance in the direction normal to the surface is shown as the inset to Figure 11. The thicknesses of the Au and Cr layers and their scattering-length densities are in a good agreement with the X-ray and neutron-reflectivity measurements on the film-free substrate in air (for the X-ray case) and in D_2O (for neutron reflectivities). The measured thickness of the film produced by the single touch is 20.1 Å. This value is consistent with the calculated length of a fully extended *all-trans* C15–

4Py molecule that is 20.6 Å. Apparently, a monolayer is formed when the single-touch procedure is employed to deposit the film. The thickness of the film produced by the double-touch method is 31 Å.

This thickness corresponds to the bilayer of the *all-trans* C15–4Py molecules that are tilted by approximately 40° from the interface normal. It may also correspond to a bilayer of C15–4Py molecules that has disordered alkyl chains (i.e. in a liquid crystalline state). The calculated scattering-length density for densely packed $(\text{CH}_2)_n$ hydrocarbon chains is approximately $-0.4 \times 10^{-6} \text{ \AA}^{-2}$. In the case of the single-touch film the value of the fitted scattering-length density for the C15–4Py (Table 1) is significantly larger. The differences between the calculated and the measured scattering-length densities suggest that the monolayer is quite loose and occupies only 72% of the electrode surface. For the bilayer, the calculated and the measured scattering-length densities agree very well. This behavior indicates that the bilayer consists of a very densely packed hydrogenated layer that occupies almost 100% of the electrode surface. In conclusion, neutron-reflectivity experiments confirm that the film of C15–4Py produced by the double-touch procedure is a bilayer. The differential-capacity and charge-density curves measured for the gold electrode covered with the films produced by the double-touch method and by the spontaneous transfer of surfactants from the G–S to the M–S interface are very similar. This similarity may be taken as evidence that the bilayer is formed by the spontaneous transfer of surfactant molecules across the triple-phase line as well. The spontaneous formation of a bilayer of C15–4Py molecules is certainly consistent with the magnitude of the critical packing parameter (cpp) for the C15–4Py molecule defined as $v/a_0 l_c$, where v is the volume occupied by the alkyl chain of the molecule, a_0 is the area of the headgroup, and l_c is the length of the alkyl chain. For C15–4Py the $\text{cpp} = 0.7$, and according to Israelachvili,²³ surfactants with this cpp should aggregate to form a bilayer at the metal–solution interface.

Summary and Conclusions

We have demonstrated that C15–4Py molecules spread at the G–S interface may flow to the M–S interface across the triple-phase line formed where the solid, liquid, and gas phases are in contact. The transfer of the surfactant molecules from the G–S to the M–S interface results in a spontaneous formation of a bilayer at the M–S interface. The formation of the bilayer is an irreversible process. Once transferred to the M–S interface, the surfactant molecules do not move back to the film-free G–S interface. We have investigated the formation of the bilayer due to the transfer of C15–4Py molecules to the gold surfaces, one that was surfactant-free and another that had been precoated with the monolayer of the surfactant molecules. Despite significant differences in the properties of the surfactant-free and the monolayer-precoated gold surfaces, similar flow rates were observed in the two cases. Two transfer mechanisms, involving either a viscous flow of a monolayer-thick slab of surfactant or lateral diffusion, were used to analyze the kinetic data. The two mechanisms predict similar time dependence for the extent of the bilayer formation. In addition, the analysis of the kinetic data gives reasonable values of both the flow rates and the diffusion coefficients. However, these two mechanisms do not explain the irreversibility of the surfactant transfer

(23) Israelachvili, J. In *Physics of Amphiphiles: Micelles, Vesicles and Microemulsions*; DeGiorgio, V., Corti, M., Eds; Elsevier Sciences Publishers: New York, 1985; p 24.

Table 1. Scattering-Length Densities and Thicknesses of the Three Layers at the Interface between the Quartz Crystal and the Electrolyte Solution^{a-e}

C15-4Py		gold layer		chromium layers				σ [Å]	χ^2
scattering-length density [10^{-6} \AA^{-2}]	thickness [Å]	scattering-length density [10^{-6} \AA^{-2}]	thickness [Å]	scattering-length density [10^{-6} \AA^{-2}]	thickness [Å]	scattering-length density [10^{-6} \AA^{-2}]	thickness [Å]		
		film obtained using the double-horizontal touching deposition							
-0.5 (0.1)	31 (2)	4.40 (0.05)	103 (2)	3.2 (0.1)	24 (2)	3.7 (0.1)	36 (2)	5.2 (0.2)	1.49
		film obtained using the single-horizontal touching technique							
1.53 (0.07)	20.1 (0.5)	4.67 (0.03)	74.4 (0.2)	3.82 (0.04)	8.9 (0.2)	3.27 (0.03)	20.7 (0.3)	5.8 (0.3)	9.6

^a Scattering-length density of monocrystalline quartz: $4.2 \times 10^{-6} \text{ \AA}^{-2}$. ^b Calculated scattering-length density of bulk gold: $4.67 \times 10^{-6} \text{ \AA}^{-2}$. ^c Calculated scattering-length density of bulk chromium: $3.02 \times 10^{-6} \text{ \AA}^{-2}$. ^d Calculated scattering-length density for densely packed $(\text{CH}_2)_n$ hydrocarbon chains is approximately $-0.4 \times 10^{-6} \text{ \AA}^{-2}$. This value was obtained assuming that the chain area/molecule is equal to 18 \AA^2 . ^e Scattering-length density of the C15-4Py in the double-touch case corresponds to 100% surface occupancy. The scattering-length density obtained in the case of single touch corresponds to 72% surface occupancy.

from the G-S to the M-S interface, nor do they account for the similar spreading rates for the surfactant-free and the precoated M-S interfaces. Therefore, we have also considered the spreading as a first-order surface reaction, controlled by the activation-energy barrier of the triple-phase line crossing. This third model not only gives a satisfactory description of the experimental results but also offers a better explanation of the similar spreading rates on the surfactant-free and the precoated M-S interfaces.

Acknowledgment. We gratefully acknowledge David Brown from the MST-11 division of the Los Alamos National Laboratory for an excellent job of sputtering gold on the quartz surfaces. The Manuel Lujan, Jr. Neutron Scattering Center is a national user facility funded by the

United States Department of Energy, Office of Basic Energy Sciences-Materials Science, under contract number W-7405-ENG-36 with the University of California. Our research was supported by a grant from the Natural Sciences and Engineering Research Council (NSERC) of Canada. I.B. thanks NSERC for a PG-S A scholarship, and V.Z. acknowledges the government of Ontario for an OGS scholarship.

Disclaimer. In this paper, any mention of a commercial product does not constitute an endorsement of that product, nor does it necessarily mean that the product mentioned is the best commercial product available.

LA000022Z